Materials Science and Engineering C 42 (2014) 681–690

Contents lists available at ScienceDirect

Materials Science and Engineering C

journal homepage: www.elsevier.com/locate/msec

Analytical and numerical study of diffusion-controlled drug release from composite spherical matrices

Amalia Hadjitheodorou [a,1], George Kalosakas [b,c,d,*]

[a] Physics Department, University of Patras, Rio GR-26504, Greece
[b] Materials Science Department, University of Patras, Rio GR-26504, Greece
[c] Institute of Chemical Engineering Sciences–Foundation of Research and Technology Hellas (FORTH/ICE-HT), PO Box 1414, Rio GR-26504, Greece
[d] Crete Center for Quantum Complexity and Nanotechnology, Physics Department, University of Crete, Heraklion GR-71003, Greece

ARTICLE INFO

Article history:
Received 18 December 2013
Received in revised form 12 May 2014
Accepted 9 June 2014
Available online 19 June 2014

Keywords:
Controlled drug delivery
Composite spheres
Diffusion
Mathematical modeling
Monte Carlo simulations
Stretched exponential (Weibull) function

ABSTRACT

We investigate, both analytically and numerically, diffusion-controlled drug release from composite spherical formulations consisting of an inner core and an outer shell of different drug diffusion coefficients. Theoretically derived analytical results are based on the exact solution of Fick's second law of diffusion for a composite sphere, while numerical data are obtained using Monte Carlo simulations. In both cases, and for the range of matrix parameter values considered in this work, fractional drug release profiles are described accurately by a stretched exponential function. The release kinetics obtained is quantified through a detailed investigation of the dependence of the two stretched exponential release parameters on the device characteristics, namely the geometrical radii of the inner core and outer shell and the corresponding drug diffusion coefficients. Similar behaviors are revealed by both the theoretical results and the numerical simulations, and approximate analytical expressions are presented for the dependencies.

© 2014 Elsevier B.V. All rights reserved.

1. Introduction

Composite matrices are increasingly gaining interest in the field of controlled drug delivery and their future pharmaceutical potentials are expected to be vast. Several studies have already been carried out for composite beads [1,2], multi-layer tablets [3] and capsules [4], core/shell microspheres [5–7], composite planar layered matrices [8,9] and coated pellets [10], among others, pointing out fundamental advantages over their conventional monolithic counterparts. For instance, composite matrices can be used for sequential release of more than one drug at a time, or to avoid chemical incompatibilities of their formulation components by physically separating them with an inert barrier [11]. In addition, and perhaps more importantly, composite matrices seem to be inherently advantageous in terms of achieving optimum drug release kinetics by combining layers with various release profiles, while suppressing the initial "burst effect" [9].

In this work, we focus on diffusion-controlled drug release from composite spherical devices, consisting of an inner core and an outer shell. This type of geometry, introducing additional design parameters to the formulation (i.e. relative sizes and relative drug diffusion coefficients of inner and outer structures), enriches the possibilities in terms of pharmacokinetics, controlled release rate and, ultimately, delivery performance.

Spherical carriers have long been favored in the field of drug delivery, particularly in nanoscale. Over the last few decades, an immense body of literature has accumulated on drug delivery devices with spherical or spherical-like morphology, such as nanoparticles [12], liposomes [13–15], polymersomes [16], dendrimers [17] and lipoproteins [18]. Most of the aforementioned systems consist of areas of different diffusion coefficients and some can be conceptualized as composite spherical carriers, a realization which renders the present study widely relevant.

The development and optimization of pharmaceutical products are greatly facilitated by mathematical models [19]. Theoretical modeling of drug delivery significantly improves the understanding of the underlying physical mechanisms governing drug release, while helping to determine the crucial parameters that regulate release rates. Moreover, the predictability offered by mathematical models reduces the number of required experiments, saving time and curtailing costs. With this in mind, we use here both theoretical and numerical models to quantify drug release kinetics from composite spherical formulations.

Several expressions have been proposed for the description of drug release, such as the Higuchi law [20], the power-law or Peppas model [21–23] and, more recently, a relatively simple formula containing a

* Corresponding author at: Materials Science Department, University of Patras, Rio GR-26504, Greece. Tel.: +30 2610 969930; fax: +30 2610 969368.
E-mail address: georgek@upatras.gr (G. Kalosakas).
[1] Currently: Department of Engineering Science, University of Oxford, Parks Road, Oxford OX1 3PJ, UK.

http://dx.doi.org/10.1016/j.msec.2014.06.009
0928-4931/© 2014 Elsevier B.V. All rights reserved.

stretched exponential function, also known as the Weibull function, Eq. (1) [24]

$$\frac{M_t}{M_\infty} = 1 - \exp\left(-\alpha t^b\right) \tag{1}$$

where α and b are constants and M_t and M_∞ are the cumulative amounts of drug released at time t and infinite time, respectively.

Eq. (1) adequately fits the entire release kinetics and has been successfully tested against a large set of experimental release data [25] as well as numerous release curves obtained numerically through Monte Carlo simulations [24,26–32]. However, when expressed in this form, parameter α of Eq. (1) has units which depend on exponent b (its units are inverse time in a non-integer power b) and thus cannot correspond to any physical quantity. This drawback prompted the suggestion for an alternative and more natural way of using the stretched exponential function [33] which reads

$$\frac{M_t}{M_\infty} = 1 - \exp\left[-\left(\frac{t}{\tau}\right)^b\right] \tag{2}$$

The form of Eq. (2) is preferred over that of Eq. (1) since the newly introduced parameter τ, has a consistent unit of time and can also be compared to other natural time scales of the controlled release problem.

Here, we discuss drug release from composite spherical matrices, when diffusion is the dominant release mechanism. Cases where other mechanisms may be present, such as degradation or swelling, are frequently encountered. Nevertheless, diffusion always emerges as a release mechanism and takes place at varying degrees in all release processes. Various drug delivery models addressing the degradation [34] and swelling [35] mechanisms have been proposed. In our model, we can also incorporate such mechanisms by introducing additional parameters but, as a first step, we present here a thorough investigation of drug release considering only diffusion; we can examine the effects of other mechanisms in future studies.

Hence, in this work we numerically calculate release profiles from composite spheres using Monte Carlo simulations. The dependence of diffusion-controlled release curves on the characteristics of the drug delivery device is investigated in detail by fitting the numerically obtained release profiles with Eq. (2) and presenting at a quantitative level the variations of parameters τ and b on the geometrical features and the drug diffusion coefficients. The acquired results are compared with predictions derived from the exact analytical solution of Fick's second law of diffusion for composite spherical systems with an initial homogeneous particle concentration. To our knowledge, the analytical fractional release profile for this case (see Eq. (3) below), has not yet been presented in the drug delivery literature.

2. Methods

In this section, we first present the exact analytical release profile obtained by the solution of Fick's second law of diffusion for a composite spherical matrix, followed by a detailed description of the Monte Carlo algorithm used in our numerical investigation.

2.1. Analytical solution of Fick's second law of diffusion for composite spherical carriers

We assume a composite sphere of radius R_2, consisting of an inner core, $0 \le r < R_1$, and an outer shell, $R_1 \le r < R_2$, with drug diffusion coefficients D_1 and D_2, respectively. Supposing that initially the formulation has a homogeneous drug concentration, C_0, using sink boundary conditions the solution of Fick's second law of diffusion yields for the fractional drug release:

$$\frac{M_t}{M_\infty} = 1 - \frac{6}{R_r^2}\sum_{n=1}^{\infty}\frac{\varphi_1(y_n)}{\varphi_2(y_n)}\exp\left(-\frac{D_1 y_n^2}{R_1^2}t\right) \tag{3}$$

where $R_r = R_2/R_1, k = \sqrt{D_1/D_2}$,

$$\varphi_1(y_n) = \frac{1}{y_n}\left(\sin^2 y_n - \frac{y_n}{2}\sin 2y_n\right)\sin[ky_n(R_r-1)] + \frac{1}{k}\left\{R_r - \frac{1}{ky_n}\sin[ky_n(R_r-1)] - \cos[ky_n(R_r-1)]\right\}\sin^2 y_n,$$

$$\varphi_2(y_n) = ky_n{}^2\sin^2[ky_n(R_r-1)] + ky_n{}^2(R_r-1)\sin^2 y_n + \frac{1-k^2}{k}\sin^2 y_n \sin^2[ky_n(R_r-1)],$$

and the sum in Eq. (3) is over the positive roots y_n of

$$ky\cot[ky(R_r-1)] + k^2 y\cot y + \left(1-k^2\right) = 0. \tag{4}$$

It is pertinent to specify here that the above solution stands when $k(R_r - 1)$ is irrational. If $k(R_r - 1)$ is rational, assuming its lowest terms as equal to l / m, the fractional release solution, Eq. (3), acquires an additional term on the right-hand side, which reads

$$-\frac{6}{\pi^2 R_r^2(lk+m)}\sum_{n=1}^{\infty}\frac{1}{n^2}\left\{\frac{(-1)^{mn+(l+m)n}}{m} + \frac{k(R_r-1)\left[R_r-(-1)^{nl}\right]}{l}\right\}\times\exp\left(-\frac{D_1 m^2 n^2 \pi^2}{R_1^2}t\right). \tag{5}$$

The derivation of the presented solution is outlined in the Appendix.

2.2. Monte Carlo algorithm used in numerical simulations

In order to simulate diffusion from a composite sphere of radius R_2, consisting of an inner core, $0 \le r < R_1$, and an outer shell, $R_1 \le r < R_2$ for various diffusion coefficient pairs (D_1, D_2), we follow a similar procedure like that used in previous studies [24,32].

We first consider a cubic lattice of size $L \times L \times L$, where $L = 2R_2$, and define a spherical region of radius R_2 inside it. Assuming a Cartesian coordinate system with origin at the center of the $L \times L \times L$ lattice, we denote x, y and z as the three coordinates that uniquely define a lattice site and consider that only sites lying inside the composite sphere $(x^2 + y^2 + z^2 < R_2^2)$ can host particles. Next, we proceed by placing a number of drug particles randomly on the sites of the composite sphere, avoiding double occupancy (assuming excluded volume interactions) until a fixed particle concentration C_0 is reached. All the numerical results presented below correspond to $C_0 = 0.5$, meaning that only 50% of the composite sphere sites are initially occupied by drug particles. In a previous study [32], we saw that release results are independent of initial concentration, which is consistent with other studies [24]. This finding was also verified here by examining several indicative cases.

Since our release device is not uniform, but consists of two areas (inner core and outer spherical shell) of interchangeable higher and lower diffusion coefficients, $D_h = \max(D_1, D_2)$ and $D_l = \min(D_1, D_2)$, respectively, we introduce a parameter denoted as q $(0 \le q < 1)$ related to the diffusivity ratio $D_r = D_l / D_h$, as $q = 1 - D_r$. Hence, when $q = 0$ we have the limiting case of diffusive motion in a uniform spherical release device (which has been studied in detail in Ref. [32]), whereas a non-zero value of q allows us to simulate diffusion processes in composite systems with different diffusion coefficients.

Diffusion is simulated by randomly selecting a drug particle at each Monte Carlo step. If the particle is located in a higher diffusion

coefficient area, we try to move it to a randomly selected nearest neighboring site. However, if the particle lies in the lower diffusion coefficient area it may stay immobile with a probability q, or we try to move it to a randomly selected nearest neighboring site with a probability $1 - q$ (this is practically done by drawing a random number in the region [0,1); the move is attempted if it is greater than or equal to q). In both cases, the potential move is allowed if the destination site is empty but rejected if already occupied, in accordance with our hypothesis of excluded volume interactions. As soon as a particle migrates to a site lying outside of the composite sphere, i.e. when $x^2 + y^2 + z^2 \geq R_2^2$, it is removed from the system.

At each Monte Carlo step, time is incremented by $1 / N(t)$, $N(t)$ being the number of drug particles still remaining in the system. We follow the number of remaining particles as a function of time until the composite sphere is completely empty. The results are statistically averaged over 100 different realizations, using the same system parameters (initial particle concentration, geometrical features R_1, R_2 and diffusion coefficient ratio D_1/D_2), but different initial random distributions of drug particles inside the composite sphere and different sequences of random numbers.

We should state here that in our numerical investigation, inner and outer radius values are given in units of the lattice spacing determining the sites of the $L \times L \times L$ cubic lattice, discussed above. In our simulation model, this lattice spacing constitutes the length unit, l_u, which can be considered to be of the order of the linear dimensions of drug particles or a larger, coarse-grained length scale, but in any case much smaller than the size of the release matrix. Accordingly, the time unit t_u of the system, being the mean time required for a drug particle to move between two neighboring lattice sites, is related to l_u through the average velocity (at the appropriate length scale), v_{dif}, of the diffusive particles as $t_u = l_u / v_{dif}$. Hence, in our Monte Carlo simulations, quantities representing length (such as the outer and inner radii of the examined composite spheres) are expressed in units of l_u and all quantities representing time (such as Monte Carlo time and parameter τ of Eq. (2) when derived from fitting numerical data) are expressed in units of t_u. Lastly, diffusion coefficients are expressed in units of D_0, where $D_0 = (1/6)l_u^2/t_u$ as estimated through the mean-square-displacement of a single particle performing a random walk in a three-dimensional cubic lattice (see the discussion before Eq. (11) in Section 3.3 of Ref. [32]). In Subsection 3.2 we will return to these observations.

3. Results and discussion

3.1. Theoretically and numerically obtained fractional release profiles

From a theoretical standpoint, we present fractional release curves, when $k(R_r - 1)$ is irrational, using the exact solution of Fick's second law of diffusion, Eq. (3), as a function of the dimensionless time $t_d = tD_1/R_1^2$. In this case, as seen from Eqs. (3) and (4), release kinetics depends on two dimensionless parameters: $R_r = R_2 / R_1$ and D_1/D_2 (or, equivalently, $k = \sqrt{D_1/D_2}$). Representative release curves obtained analytically are depicted with symbols in Fig. 1a for a fixed size ratio of $R_2 / R_1 = 2$ and various D_1/D_2 values, and in Fig. 2a for a fixed drug diffusion coefficient ratio of $D_1 / D_2 = 5$ and different values of R_2/R_1.

In order to compare the theoretical predictions regarding release profiles from composite spherical formulations with the numerically obtained results, we fit the analytical fractional release curves with the stretched exponential kinetics of Eq. (2) (solid curves in Figs. 1a and 2a). The following methodology was used for these fits: a characteristic dimensionless time $t_0 = 1/y_1^2$ was set, y_1 being the first root of Eq. (4), and theoretical data were obtained from Eq. (3) up to a dimensionless time $t_{max} = 10t_0$, recorded at equidistant steps of $t_0/100$. These theoretical data were then fitted with Eq. (2). A similar methodology was also implemented in a previous study [32] in order to fit the analytical fractional release curve for a simple homogeneous sphere. The only difference was that the characteristic dimensionless time was then set as $t_0 = 1 / \pi^2$ due to the form of the analytical solution of Fick's second law of diffusion in that case (see Eq. (4) in Ref. [32]).

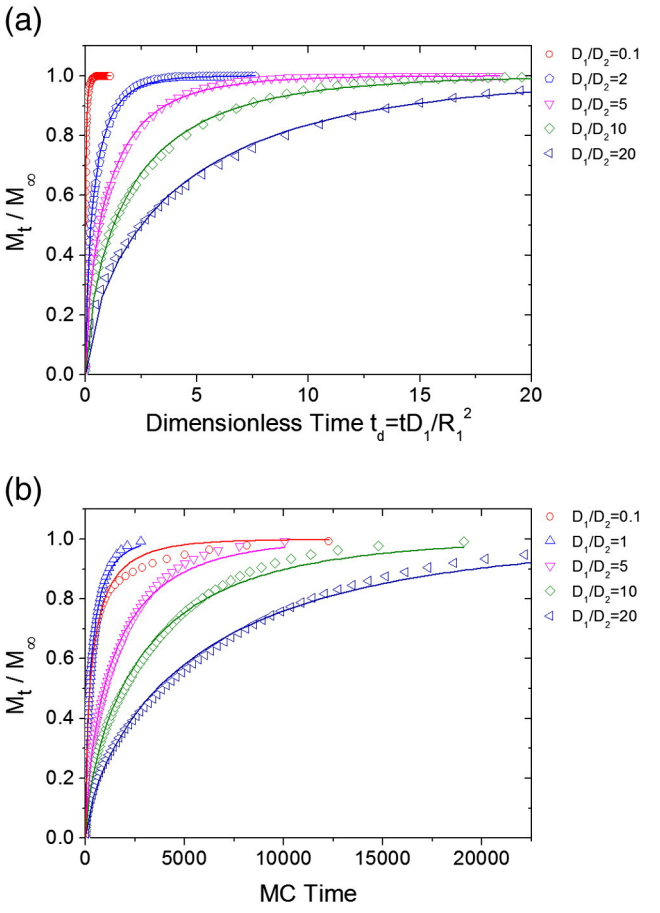

Fig. 1. (a) Theoretical fractional drug release curves derived from the exact solution of Fick's second law of diffusion for composite spheres, Eq. (3), for fixed size ratio $R_2/R_1 = 2$ and $D_1/D_2 = 0.1, 2, 5, 10, 20$ (open symbols). (b) Numerically obtained fractional release curves, M_t/M_∞, versus Monte Carlo time for composite spheres of outer radius $R_2 = 32$, inner radius $R_1 = 16$ and $D_1/D_2 = 0.1, 1, 5, 10, 20$ (open symbols). The initial concentration of drug particles, homogeneously distributed in the inner and outer structure, is $C_0 = 0.5$ in all numerical simulations. Solid curves, in both (a) and (b), are fits with the stretched exponential function, Eq. (2).

From a numerical standpoint, we ran a number of Monte Carlo simulations, as described in Subsection 2.2, to investigate the dependence of release kinetics from the size and diffusion coefficient ratios of composite spherical devices. We examined composite spheres with a homogeneous initial drug concentration $C_0 = 0.5$, of outer radius $R_2 = 32l_u$ and R_2/R_1 ratios ranging from 1 to 8. Composite spherical carriers of larger and smaller outer radius values R_2 were also examined yielding similar results to those presented here, apart from some cases (for particular values of R_2/R_1 and D_1/D_2) in relatively small formulations with $R_2 \sim 15l_u$ which may represent small size effects. Regarding the relative drug diffusion coefficients, we examined cases where values of D_1/D_2 ranged from 0.05 to 20, including cases where $k(R_r - 1)$ was rational, in order to indentify whether they exhibit a different qualitative dependence; all cases were found to generate results that showcased the same behaviors and were therefore smoothly incorporated into continuous figures.

Release curves numerically obtained through Monte Carlo simulations, like those indicatively shown with symbols in Figs. 1b and 2b, were also fitted with the stretched exponential function, Eq. (2), which was found to describe the entire release profile (see solid curves

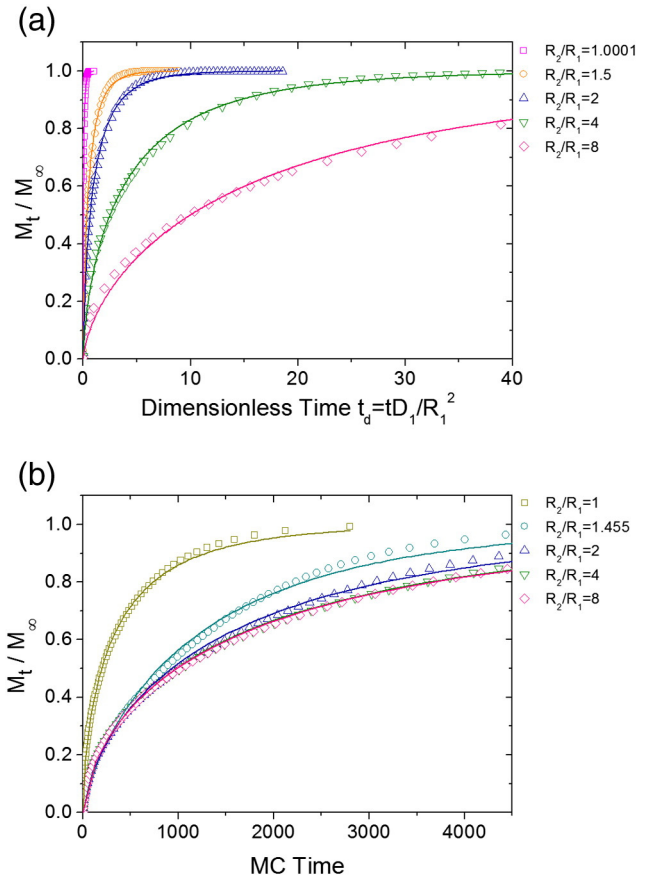

Fig. 2. (a) Theoretical fractional drug release curves derived from the exact solution of Fick's second law of diffusion for composite spheres, Eq. (3), for fixed diffusion coefficient ratio $D_1/D_2 = 5$ and $R_2/R_1 = 1.0001, 1.5, 2, 4, 8$ (open symbols). (b) Numerically obtained fractional release curves, M_t/M_∞, versus Monte Carlo time for composite spheres of outer radius $R_2 = 32$, inner and outer diffusion coefficients $D_1 = 1$ and $D_2 = 0.2$, respectively, and inner radius values $R_1 = 32, 22, 16, 8, 4$ (open symbols). The initial concentration of drug particles, homogeneously distributed in the inner and outer structure, is $C_0 = 0.5$ in all numerical simulations. Solid curves, in both (a) and (b), are fits with the stretched exponential function, Eq. (2).

in Figs. 1b and 2b), in accordance with previous studies [24,27–30,32]. Some relatively small deviations of the fitting were observed for the smallest investigated values of D_1/D_2 (0.05 and 0.1) and for intermediate values of size ratio ($1.14 \le R_2/R_1 \le 1.46$). However, even for these cases, Eq. (2) exhibits the correct asymptotic behavior (saturation at unity) at relatively large times, providing quite a good overall description of the numerically obtained data.

In terms of comparison between the corresponding theoretical and numerical fractional releases shown in Figs. 1a, b and 2a, b the reader should note that in the theoretical cases, x-axis depicts the dimensionless time tD_1/R_1^2. If one plots the numerical data as a function of Monte Carlo time multiplied by D_1/R_1^2, the release curves will reorder in a manner similar to that exhibited by the corresponding theoretical ones. Here, however, we show the numerical results in Figs. 1b and 2b as a function of Monte Carlo time since these were the raw data used for the fittings with the stretched exponential release Eq. (2).

Parenthetically, we should point out that numerical fractional release curves do not depend on C_0. Indeed, for fixed size and drug diffusion coefficient ratios, the numerically obtained release curves for $C_0 =$ 0.1, 0.5 and 0.9 were non-distinguishable. This is in accordance with the theoretical prediction of the analytical solution of the diffusion equation (ignoring inter-particle interactions) and with Monte Carlo simulations of drug release from simple cylindrical and spherical devices presented in Refs. [24] and [32], respectively.

Fitting both the analytically and numerically obtained release curves with Eq. (2), we calculate the dependence of the stretched exponential parameters τ and b on the characteristics of the composite spherical carrier, namely the radii of the inner core and outer shell (R_1 and R_2) and the corresponding drug diffusion coefficients (D_1 and D_2). The derived dependencies of τ and b are presented in Subsections 3.2 and 3.3, respectively.

3.2. Dependence of the stretched exponential parameter τ on the geometrical characteristics and the drug diffusion coefficients

Parameter τ of the stretched exponential function, Eq. (2), is a time parameter and, as such, it is expressed in units of time. In the analytical release curves presented above, we considered the dimensionless time $t_d = tD_1/R_1^2$, meaning that time was measured in units of R_1^2/D_1. Therefore, in our analytical investigation, by fitting the exact solution of Fick's second law of diffusion, Eq. (3), with the stretched exponential function (following the procedure recounted in Subsection 3.1), we obtained the dimensionless values $\tau_d = \tau D_1/R_1^2$ of the stretched exponential parameter τ.

However, the numerical release curves are plotted versus Monte Carlo time, measured in units of t_u (mean time required for a particle to move between neighboring lattice sites). Hence, to acquire the corresponding numerical τ_d values, comparable to the analytically derived ones discussed previously, we have to divide the stretched exponential time parameters resulting from the fittings of the numerical release profiles with Eq. (2), by a similar factor $\propto R_1^2/D_1$. Thus, since in our simulation model the radius R_1 has units of l_u and the drug diffusion coefficient D_1 units of $D_0 = (1/6)l_u^2/t_u$, to enable a direct comparison between the analytical and the numerical τ_d values we divide the numerically acquired fitting results by the factor $6R_1^2/D_1$. This factor of 6, resulting from the considered unit system, was also used for comparing numerical and theoretical results of the stretched exponential parameter τ in the case of homogeneous spheres [32].

Fig. 3a and b shows the variation of the dimensionless stretched exponential parameter τ_d with the drug diffusion coefficient ratio D_1/D_2, derived from the analytical and the numerical approach, respectively. Different symbols represent different values of size ratio R_2/R_1 (as shown on the right-hand side of each plot). A linear dependence of τ_d on D_1/D_2 is depicted in both figures.

A linear dependence of parameter τ_d is also evident when plotting τ_d versus $(R_2/R_1)^2$. The theoretical and numerical results can be seen in Fig. 4a and b, respectively, where different symbols correspond to different values of the diffusion coefficient ratio D_1/D_2.

Based on these observations and taking into consideration the limiting case of the simple homogeneous sphere (resulting here when $R_2 = R_1$ or $D_1 = D_2$) the following relation is suggested:

$$\tau_d = c\left[1 + \frac{D_1}{D_2}\left(\frac{R_2^2}{R_1^2} - 1\right)\right] \tag{6}$$

where $c = 0.054$ for the theoretical results and $c = 0.058$ for the numerical ones [32].

In Figs. 3a and 4a we have plotted this formula along with the theoretical values of τ_d, as derived from the analytical investigation. As seen, the above relation describes the data very well. Restoring normal units, in other words taking into account that $\tau = \tau_d R_1^2/D_1$, we obtain

$$\tau = 0.054\left(\frac{R_1^2}{D_1} + \frac{R_2^2 - R_1^2}{D_2}\right), \quad \text{independent of } C_0\,. \tag{7}$$

Turning to the numerical calculations, plots of Eq. (6) having $c =$ 0.058 along with the numerically acquired values of τ_d are presented

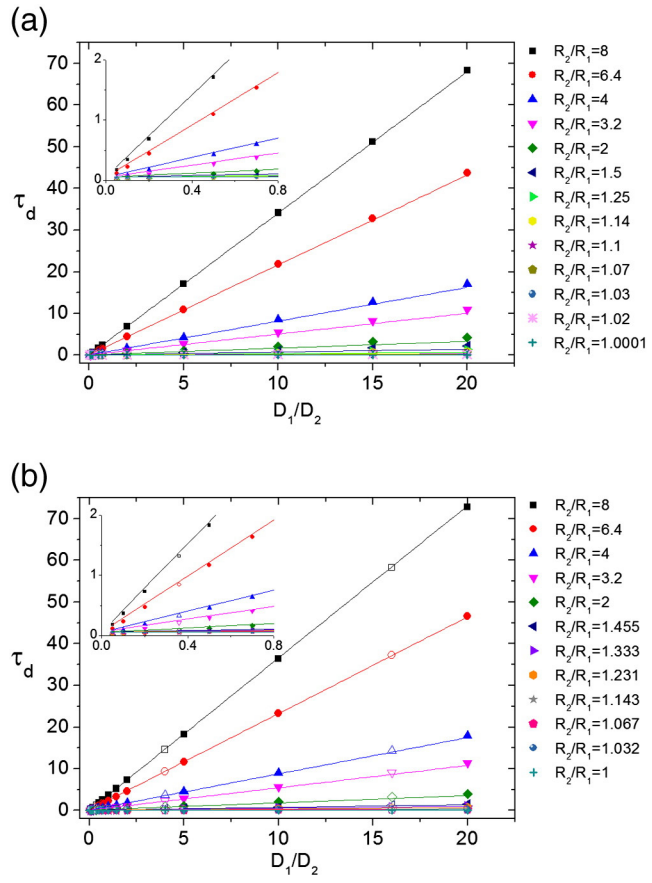

Fig. 3. (a) Theoretically and (b) numerically derived dimensionless time parameter $\tau_d = \tau D_1/R_1^2$ of the stretched exponential release, Eq. (2), as a function of D_1/D_2 for different values of the geometrical ratio R_2/R_1 (symbols). Plots of Eq. (6) with $c = 0.054$ in (a) and $c = 0.058$ in (b) are shown by solid lines. Solid symbols in (b) correspond to cases where $k = \sqrt{D_1/D_2}$ is irrational and open symbols to cases where k is rational. Insets show a magnification of the plots in the $D_1 < D_2$ region.

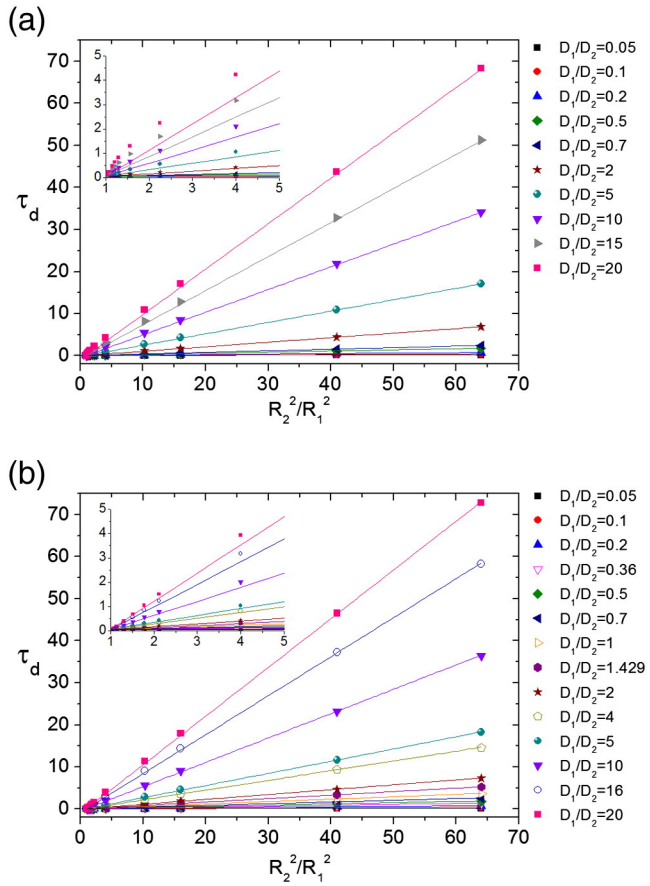

Fig. 4. (a) Theoretically and (b) numerically derived dimensionless time parameter $\tau_d = \tau D_1/R_1^2$ of the stretched exponential release, Eq. (2), as a function of $(R_2/R_1)^2$, for different values of the drug diffusion coefficients ratio D_1/D_2 (symbols). Plots of Eq. (6) with $c = 0.054$ in (a) and $c = 0.058$ in (b) are shown by solid lines. Solid symbols in (b) correspond to cases where $k = \sqrt{D_1/D_2}$ is irrational and open symbols to cases where k is rational. Insets show a magnification of the plots for the smaller values of R_2/R_1.

in Figs. 3b and 4b. Once again, data are described very well by the relation suggested. Multiplying τ_d by R_1^2/D_1, we obtain the following relation in normal units for the stretched exponential parameter τ:

$$\tau = 0.058\left(\frac{R_1^2}{D_1} + \frac{R_2^2 - R_1^2}{D_2}\right), \quad \text{independent of } C_0\,. \tag{8}$$

From Eqs. (7) and (8) we see that the theoretical dependence (derived from the analytical solution of the diffusion equation) of the stretched exponential time parameter τ on the characteristics of the composite carrier is in quantitative agreement with the numerical one (obtained through Monte Carlo simulations). For the limiting cases of $R_1 = R_2 = R$ or $D_1 = D_2 = D$, Eqs. (7) and (8) reduce to relations presented earlier (see Eqs. (6) and (11), respectively, in Ref. [32]) regarding diffusion-controlled drug release from simple spherical formulations.

As mentioned in a previous study [32], a process exhibiting a stretched exponential time dependence can be described by an average characteristic time τ^{av} obtained through the relation $\tau^{av} = \frac{\Gamma(1/b)}{b}\tau$, where $\Gamma(1/b)$ is the gamma function with argument $1/b$. The smaller the exponent b, the larger the τ^{av} as compared to τ. Plugging the acquired values of τ_d and b into this relation, we have calculated the dimensionless average characteristic times, τ_d^{av}, describing the release process from a composite spherical matrix. The variations of τ_d^{av} with D_1/D_2 and $(R_2/R_1)^2$ obtained from a numerical standpoint are presented in Fig. 5a and b, respectively. Insets on said figures present the corresponding variations of the theoretical results.

3.3. Dependence of the stretched exponential parameter b on the geometrical characteristics and the drug diffusion coefficients

The dependence of the stretched exponential exponent b on the drug diffusion coefficient ratio D_1/D_2 as derived from fitting the analytical and the numerical release curves with Eq. (2) is presented in Fig. 6a and b, respectively. Different symbols represent different values of size ratio R_2/R_1. It can be seen that b increases with D_1/D_2, reaching a saturation in most of the examined cases. Numerically obtained values of b vary between a larger range than the corresponding theoretical ones.

Plotted results can be approximated with a function of the form $b = y_0 + A\left[1 - \exp\left(-\frac{(D_1/D_2)-1}{B}\right)\right]$. For $D_1 = D_2$ this relation yields $b = y_0$, thus y_0 can be determined by considering the expressions that provide the stretched exponential parameter b in the limiting case of the simple spherical carrier studied in Ref. [32]. Indeed, the analytical investigation of diffusion-controlled drug release from simple spherical formulations yielded $b = 0.68$ whereas numerically, b was found to follow the relation $b = \frac{1.0}{R/l_u} + 0.61$ (see Eqs. (5) and (13), respectively, in Ref. [32]).

Therefore, the analytically derived data, presented in Fig. 6a, are fitted with

$$b = 0.68 + A\left[1 - \exp\left(-\frac{(D_1/D_2)-1}{B}\right)\right] \tag{9}$$

and the numerically acquired results, depicted in Fig. 6b, are fitted

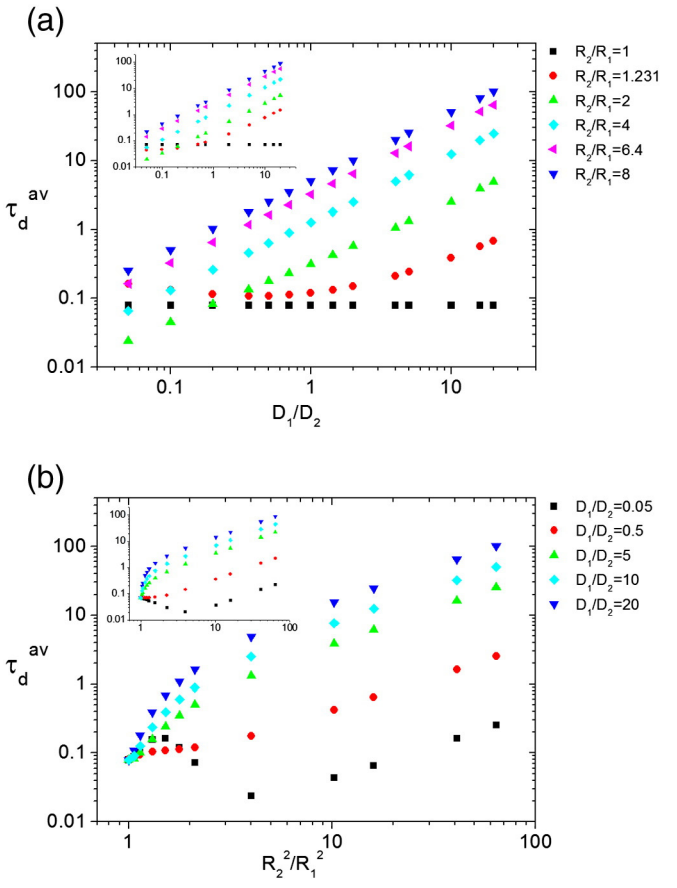

Fig. 5. Dimensionless average characteristic time τ_d^{av} obtained from the numerical simulations (a) as a function of the drug diffusion coefficients ratio D_1/D_2, for different values of R_2/R_1 and (b) as a function of $(R_2/R_1)^2$ for different values of D_1/D_2. Insets exhibit the corresponding dependences as derived from the theoretical investigation. Same symbols in main graphs and insets correspond to same parameter values, except for two cases in the inset of (a) where squares correspond to $R_2/R_1 = 1.001$ and cycles to $R_2/R_1 = 1.25$.

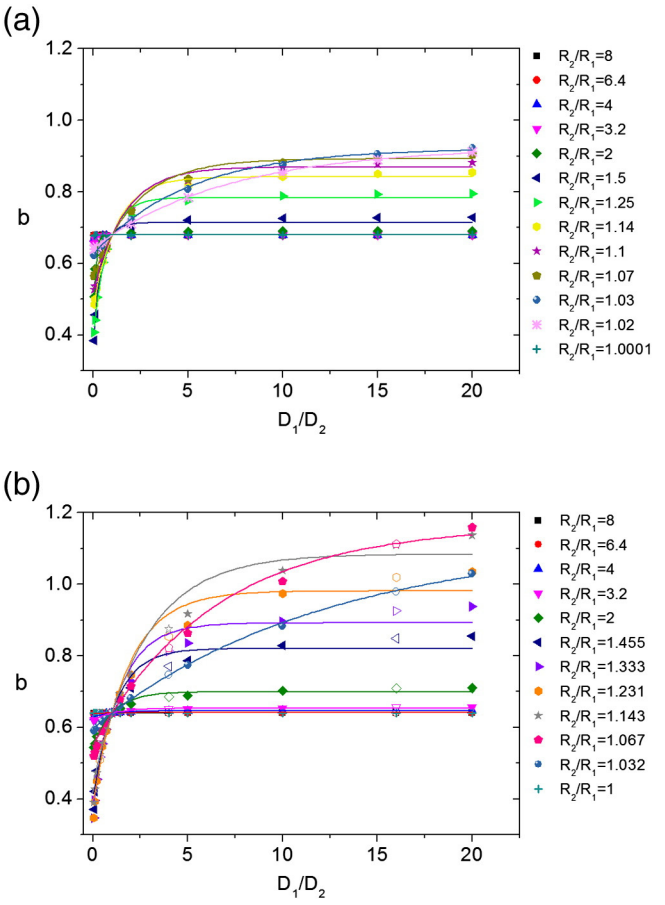

Fig. 6. (a) Theoretically and (b) numerically derived exponent b of the stretched exponential release, Eq. (2), as a function of the drug diffusion coefficient ratio D_1/D_2, for different values of R_2/R_1 (symbols). Solid curves show fits with Eq. (9) in (a) and with Eq. (10), having set $R_2 = 32l_u$, in (b). Solid symbols in (b) correspond to cases where $k = \sqrt{D_1/D_2}$ is irrational and open symbols to cases where k is rational.

with

$$b = 0.61 + \frac{1.0}{R_2/l_u} + A\left[1 - \exp\left(-\frac{(D_1/D_2)-1}{B}\right)\right] \tag{10}$$

after substituting R_2 with the outer radius value of our examined composite spherical carriers, namely $R_2 = 32l_u$. The aforementioned fittings are depicted by solid curves in Fig. 6a and b.

In order to derive an approximate relation for the dependence of b on the geometrical characteristics of the composite device, we examine the variations of the fitting parameters A and B of Eqs. (9) and (10) with the size ratio R_2/R_1. The resulting fitting parameters A and B of Eq. (9) are plotted in Fig. 7a and b versus R_2/R_1. Similar dependencies are obtained for the parameters A and B of Eq. (10) as regards the numerical data. In both cases, the decreasing functions of A and B with R_2/R_1 are approximated by Eqs. (11) and (12), respectively.

$$A = G_1 \exp\left[-\frac{(R_2/R_1)-1}{G_2}\right] \tag{11}$$

$$B = \frac{F_1}{\left(\ln\frac{R_2}{R_1}\right)^{F_2}} \tag{12}$$

The corresponding fittings for the theoretical results are shown with solid curves in Fig. 7a and b, yielding $G_1 = 0.27$, $G_2 = 0.26$, $F_1 = 0.19$ and $F_2 = 0.92$. Similar fits of parameters A and B of Eq. (10) for the numerical results give $G_1 = 0.57$, $G_2 = 0.43$, $F_1 = 0.58$ and $F_2 = 0.88$.

Therefore, at a quantitative level, summarizing the approximate dependencies of the stretched exponential parameter b on the size and drug diffusion coefficient ratios, we get the rather complicated relations

$$b = 0.68 + 0.27\exp\left[-\left(\frac{\frac{R_2}{R_1}-1}{0.26}\right)\right]\left\{1 - \exp\left[-\left(\frac{\left(\frac{D_1}{D_2}-1\right)\left(\ln\frac{R_2}{R_1}\right)^{0.92}}{0.19}\right)\right]\right\} \tag{13}$$

from the analytical approach and

$$b = 0.61 + \frac{1}{R_2/l_u} + 0.57\exp\left[-\left(\frac{\frac{R_2}{R_1}-1}{0.43}\right)\right] \times \left\{1 - \exp\left[-\left(\frac{\left(\frac{D_1}{D_2}-1\right)\left(\ln\frac{R_2}{R_1}\right)^{0.88}}{0.58}\right)\right]\right\} \tag{14}$$

from the numerical Monte Carlo approach. Note that in cases of practical interest, where $R_2 \gg l_u$, the second term on the right-hand side of the last equation can be ignored as compared to the other terms.

Fig. 8a and b presents our theoretical and numerical findings, respectively, regarding the dependence of exponent b of Eq. (2) on R_1/R_2 (data shown by different symbols for the various values of D_1/D_2 examined),

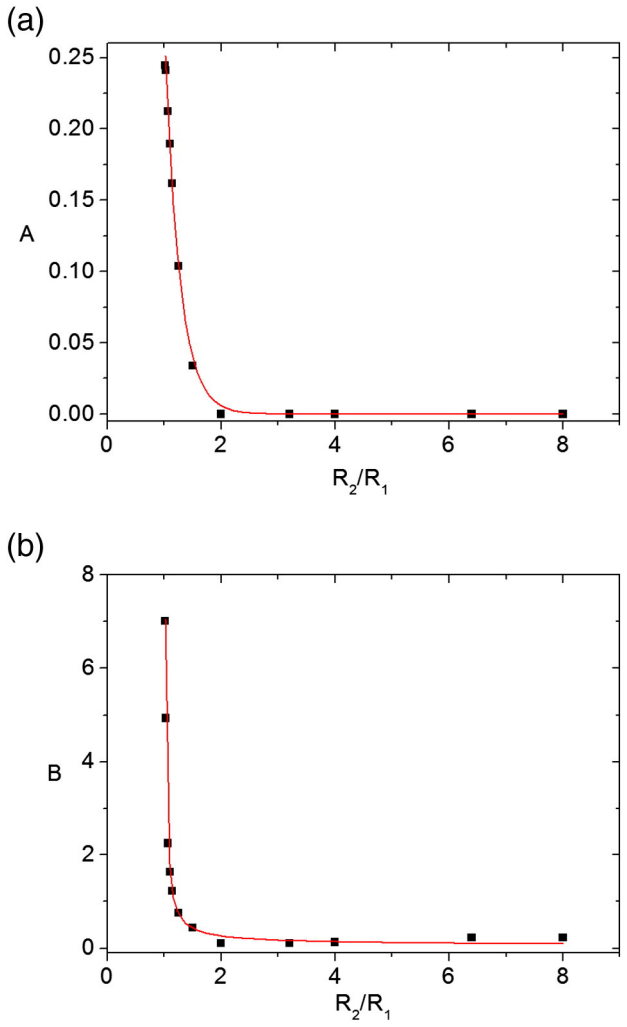

Fig. 7. Dependence of the fitting parameters (a) A and (b) B of Eq. (9) on the geometrical size ratio R_2/R_1 (symbols). Solid curves show fits with Eq. (11) in (a) and with Eq. (12) in (b).

along with the corresponding plots of Eqs. (13) and (14) (shown by solid curves). The R_1/R_2 dependence of b is particularly interesting, presenting an extremum; a maximum when $D_1/D_2 > 1$ and a minimum when $D_1/D_2 < 1$. This common behavior, exhibited by both the theoretical and the numerical results, is captured by the approximate expressions of Eqs. (13) and (14), respectively. Quantitatively, the description is more accurate for the theoretical data, especially for the smaller values of D_1/D_2 (less than 0.3).

Our analytical investigation yielded b values lying roughly between 0.4 and 0.9, whereas our numerically acquired values range from 0.3 to 1.2. A previous study [25] reported that when examining cases of diffusion in normal Euclidian space, the exponent b was found in the region between 0.69 and 0.75, while b values less than 0.69 were indicative of fractal or highly disordered spaces, and values greater than 0.75 were attributed to more complicated release mechanisms; however, diffusion-controlled release from composite matrices had not been considered. A subsequent work [29], studying a two-dimensional square lattice with a high diffusivity interior and low diffusivity thin layer around the border, found b values to be larger than 0.75, a result which is consistent with that found here for composite spheres with $D_1/D_2 > 1$.

3.4. Drug release from composite spheres with diffusion coefficients differing by a few orders of magnitude

Numerically, we have also examined release from composite spherical carriers with drug diffusion coefficient ratios D_1/D_2 in a much larger range of values covering six orders of magnitude (from 10^{-3} to 10^{3}). Cases where $D_1 \gg D_2$ are of particular interest as they are relevant to liposomal release devices that have received increased attention for drug delivery applications. Again, fittings to release data with the stretched exponential function, Eq. (2), were very good when $D_1/D_2 > 1$, but some deviations were observed for intermediate values of R_2/R_1, when $D_1/D_2 < 1$.

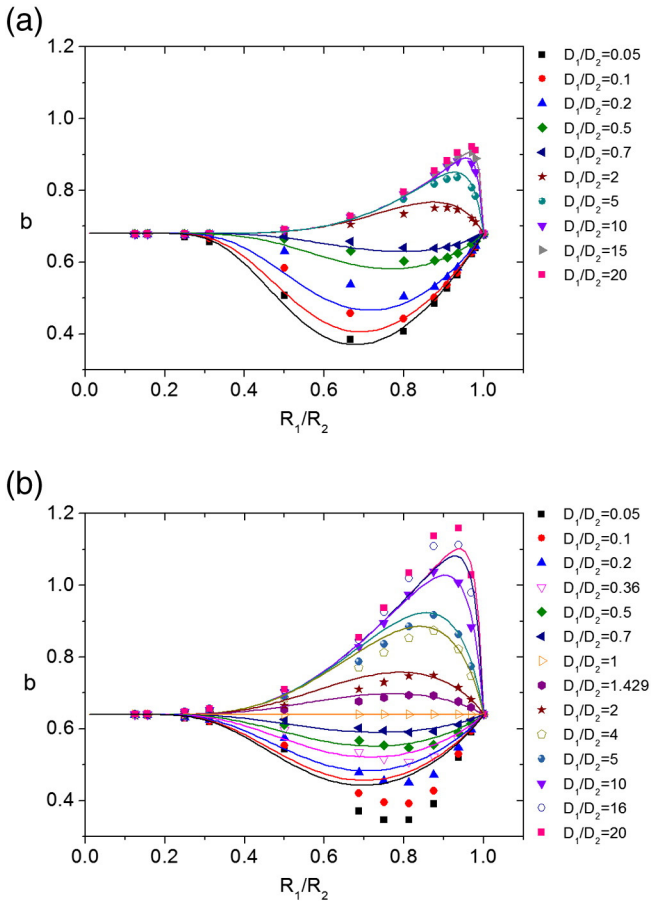

Fig. 8. (a) Theoretically and (b) numerically derived exponent b of the stretched exponential release, Eq. (2), as a function of the geometrical size ratio R_1/R_2, for different values of D_1/D_2 (symbols). Solid curves show plots of Eq. (13) in (a) and of Eq. (14) with $R_2 = 32l_u$ in (b). Solid symbols in (b) correspond to cases where $k = \sqrt{D_1/D_2}$ is irrational and open symbols correspond to cases where k is rational.

Even with extreme values of D_1/D_2 considered, the observed behavior of the stretched exponential parameter τ shows an excellent agreement with Eq. (8), exhibiting once again the theoretically anticipated behavior, as derived from the analytical solution of the diffusion equation.

As regards the exponent b of Eq. (2), qualitatively we acquire the same behavior, but the deviations from Eq. (14) are larger than those presented in Fig. 8b. Moreover, it seems that the maximum (minimum) value of b observed for $D_1/D_2 > 1$ ($D_1/D_2 < 1$) in the numerically obtained release data shows a saturation as D_1/D_2 increases (decreases) at a value around 1.5 (0.2).

4. Conclusions

Using both analytical and numerical models, we investigated diffusion-controlled drug release from composite spherical devices. The obtained fractional release curves and their dependence on the relative sizes and diffusion coefficients of the inner core and outer shell have been quantified. Release kinetics was independent of the initial drug concentration.

Theoretical predictions were drawn from the analytical solution of Fick's second law of diffusion for a composite sphere. Numerical data were obtained through Monte Carlo simulations. Both the theoretical and the numerical fractional release curves were found to be accurately described by the stretched exponential function, Eq. (2), and approximate analytical relations for the dependencies of its two parameters, τ and b on the release device characteristics have been presented.

The dimensionless stretched exponential time parameter τ_d was shown to have a linear dependence on both D_1/D_2 and $(R_2/R_1)^2$. After restoring normal units, τ is found proportional to $\left(\frac{R_1^2}{D_1}+\frac{R_2^2-R_1^2}{D_2}\right)$. The exponent b was found to increase with D_1/D_2, reaching a saturation in most of the examined cases, while its dependence on R_1/R_2 is more complicated, presenting a maximum for $D_1/D_2 > 1$ and a minimum for $D_1/D_2 < 1$.

In the limiting case of $D_1 = D_2$ or $R_1 = R_2$, the parameters τ and b derived here reduce to the corresponding values found for the case of diffusion-controlled release from simple homogeneous spherical matrices [32].

Acknowledgments

This work has been partially supported by the Thales Project MACOMSYS, co-financed by the European Union (ESF) and the Greek Ministry of Education (thought the ΕΣΠΑ program), and by the European Union's Seventh Framework Programme (FP7-REGPOT-2012-2013-1) under grant agreement no. 316165.

Appendix A

We present here the main steps in solving Fick's second law of diffusion for a composite sphere of radius R_2 (whose inner core, $0 \le r < R_1$, and outer shell, $R_1 \le r < R_2$, have diffusion coefficients D_1 and D_2, respectively) as well as the derivations of Eqs. (3) and (5). We assume a homogeneous particle concentration, C_0, at $t = 0$. Due to the spherical symmetry of the problem, drug concentration depends solely upon the distance r from the center of the composite sphere. Thus, if we denote as v_1 and v_2 the drug concentrations within the inner core and the outer shell, respectively, one has to solve the following set of equations

$$\frac{\partial(rv_1)}{\partial t} = D_1\frac{\partial^2(rv_1)}{\partial r^2}, 0 \le r < R_1, t > 0 \qquad \frac{\partial(rv_2)}{\partial t} = D_2\frac{\partial^2(rv_2)}{\partial r^2}, R_1 \le r < R_2, t > 0 \tag{A1}$$

Considering $u_1 = rv_1$ and $u_2 = rv_2$, the above equations become

$$\frac{\partial u_1}{\partial t} = D_1\frac{\partial^2 u_1}{\partial r^2}, 0 \le r < R_1, t > 0 \qquad \frac{\partial u_2}{\partial t} = D_2\frac{\partial^2 u_2}{\partial r^2}, R_1 \le r < R_2, t > 0\,. \tag{A2}$$

The continuity of the drug concentration and the balance of fluxes at the interface between the inner core and the outer shell result in

$$u_1(r = R_1) = u_2(r = R_1), \forall\, t > 0 \qquad \text{and} \qquad D_1\left(\frac{1}{r}\frac{\partial u_1}{\partial r} \partial \frac{u_1}{r^2}\right)\Big|_{r=R_1} = D_2\left(\frac{1}{r}\frac{\partial u_2}{\partial r} - \frac{u_2}{r^2}\right)\Big|_{r=R_1}, \forall\, t > 0$$

respectively.

The boundary conditions to be satisfied are $u_1(r = 0) = 0, \forall\, t > 0$, since v_1 has to be finite at $r = 0$, and $u_2(r = R_2) = 0, \forall\, t > 0$ (sink boundary conditions at the sphere external surface).

Finally, the initial conditions are $u_1(t = 0) = rC_0$ and $u_2(t = 0) = rC_0$.

Applying the Laplace transform, $\tilde{u} = \int_0 u\, e^{-pt} dt$, and setting

$$q_1^2 = p/D_1, \quad q_2^2 = p/D_2 \tag{A3}$$

we get the following subsidiary equations

$$\frac{d^2\tilde{u}_1}{dr^2} - q_1^2\tilde{u}_1 = -\frac{rC_0}{D_1}\, 0 \le r < R_1; \quad \frac{d^2\tilde{u}_2}{dr^2} - q_2^2\tilde{u}_2 = -\frac{rC_0}{D_2}\, R_1 \le r < R_2\,. \tag{A4}$$

$$\text{with} \quad \tilde{u}_1(r = 0) = 0, \quad \tilde{u}_2(r = R_2) = 0, \quad \tilde{u}_1(r = R_1) = \tilde{u}_2(r = R_1),$$
$$\text{and} \quad D_1\left(R_1\frac{d\tilde{u}_1}{dr} - \tilde{u}_1\right)\Big|_{r=R_1} = D_2\left(R_1\frac{d\tilde{u}_2}{dr} - \tilde{u}_2\right)\Big|_{r=R_1}$$

The general solutions of the differential Eqs. (A4) are

$$\tilde{u}_1 = A_1\sinh(q_1 r) + B_1\cosh(q_1 r) + \frac{rC_0}{p}, \quad 0 \le r < R_1 \tag{A5}$$

$$\tilde{u}_2 = A_2\sinh[q_2(r - R_1)] + B_2\cosh[q_2(r - R_1)] + \frac{rC_0}{p}, \quad R_1 \le r < R_2\,. \tag{A6}$$

By imposing the boundary conditions we obtain for the $\tilde{v}_i = \tilde{u}_i/r, i = 1, 2$ that

$$\tilde{v}_1 = \frac{C_0}{p} - \frac{R_1R_2C_0D_2q_2\sinh(rq_1)}{rp\{D_2\psi_2(R_2)\sinh(q_1R_1) + D_1\psi_1(R_1)\sinh[q_2(R_2 - R_1)]\}} \tag{A7}$$

$$\tilde{v}_2 = \frac{C_0}{p} - \frac{R_2C_0\{D_2\psi_2(r)\sinh(q_1R_1) + D_1\psi_1(R_1)\sinh[q_2(r - R_1)]\}}{rp\{D_2\psi_2(R_2)\sinh(q_1R_1) + D_1\psi_1(R_1)\sinh[q_2(R_2 - R_1)]\}} \tag{A8}$$

where $\psi_1(r) = R_1q_1\cosh(q_1r) - \sinh(q_1r)$, $\psi_2(r) = R_1q_2\cosh[q_2(r - R_1)] + \sinh[q_2(r - R_1)]$.

In order to evaluate v_1 and v_2 we apply the inverse Laplace transform to the above expressions of $\tilde{v}_1$ and $\tilde{v}_2$ [36]. The application to the first right-hand side (RHS) terms gives integrals whose integrands have simple poles at $\lambda = 0$, yielding contributions of C_0. Also, applying the inverse Laplace transform to the second RHS terms gives integrals whose integrands have poles of second order at $\lambda = 0$ (yielding total contributions of $-C_0$), and simple poles at $\lambda = -D_1x_m^2$, where $\pm x_m$, $m = 1, 2,\ldots$, are the roots of

$$\begin{aligned} &D_2\{kR_1x\cos[k(R_2 - R_1)x] + \sin[k(R_2 - R_1)x]\}\sin(R_1x) \\ &+D_1\{R_1x\cos(R_1x) - \sin(R_1x)\}\sin[k(R_2 - R_1)x] = 0 \end{aligned} \tag{A9}$$

and $k = \sqrt{D_1/D_2}$.

Eq. (A9) results by considering the denominator of the second RHS terms of Eqs. (A7) and (A8) equal to zero and setting $q_1 = xi$, $q_2 = kxi$ while substituting the variable p with $\lambda = -D_1x^2$ [see Eq. (A3)].

The roots of Eq. (A9) are the roots of

$$D_2\{kR_1x\cot[k(R_2 - R_1)x] + 1\} + D_1\{R_1x\cot(R_1x) - 1\} = 0 \tag{A10}$$

together with the common roots of

$$\sin(R_1x) = 0 \quad \text{and} \quad \sin[k(R_2 - R_1)x] = 0\,. \tag{A11}$$

If $k(R_2 - R_1)/R_1$ is irrational, then the $\sin(R_1x) = 0$ and $\sin[k(R_2 - R_1)x] = 0$ of Eq. (A11) have no common roots and from the expressions of $\tilde{v}_1$ and $\tilde{v}_2$ we get that

$$v_1 = \frac{2R_2C_0}{r}\sum_{n=1}^{\infty}\frac{1}{\varphi(x_n)}\sin(rx_n)\sin(R_1x_n)\sin[k(R_2 - R_1)x_n]\exp\left(-D_1x_n^2t\right) \tag{A12}$$

$$v_2 = \frac{2R_2C_0}{r}\sum_{n=1}^{\infty}\frac{1}{\varphi(x_n)}\sin^2(R_1x_n)\sin[k(R_2 - r)x_n]\exp\left(-D_1x_n^2t\right) \tag{A13}$$

where x_n, $n = 1, 2,\ldots$, are the roots of Eq. (A10), and

$$\varphi(x_n) = kR_1x_n\sin^2[kx_n(R_2-R_1)] + kx_n(R_2-R_1)\sin^2(R_1x_n) + \frac{1-k^2}{kR_1x_n}\sin^2(R_1x_n)\sin^2[kx_n(R_2-R_1)]. \tag{A14}$$

However, if $k(R_2 - R_1)/R_1$ is rational, suppose in its lowest terms it is equal to l / m then the $\sin(R_1x) = 0$ and $\sin[k(R_2 - R_1)x] = 0$ of Eq. (A11) have common positive roots

$$x = \frac{mn\pi}{R_1},\quad n = 1, 2, 3, \ldots.$$

The above roots give rise to the following additional terms

$$-\frac{2R_2C_0}{r\pi(lk+m)}\sum_{n=1}^{\infty}\frac{(-1)^{(l+m)^n}}{n}\sin\frac{mn\pi r}{R_1}\exp\left(-\frac{D_1m^2n^2\pi^2}{R_1^2}t\right) \tag{A15}$$

and

$$\frac{2R_2C_0k}{r\pi(lk+m)}\sum_{n=1}^{\infty}\frac{1}{n}\sin\frac{n\pi l(R_2-r)}{R_2-R_1}\exp\left(-\frac{D_1m^2n^2\pi^2}{R_1^2}t\right) \tag{A16}$$

in the expressions of Eqs. (A12) and (A13) for v_1 and v_2, respectively.

Moreover, the initial particle concentration equals to

$$C_0 = \frac{M_\infty}{V_{sphere}} = \frac{M_\infty}{\frac{4}{3}\pi R_2^3} \tag{A17}$$

where M_∞ denotes the total mass of the diffusive substance, the mass which exits the composite sphere in infinite time. Now, if we denote as M_t the corresponding mass of the diffusive substance which has left the matrix in time t, we have

$$M_t = M_\infty - \int\int\int v_1(r,t)dV_1 - \int\int\int v_2(r,t)dV_2\,, \tag{A18}$$

where the triple integrals over dV_1 and dV_2 are over the inner core and outer shell, respectively.

Substituting in the last equation the expressions (A12) and (A13), and using Eq. (A17), we obtain for the fractional release

$$\frac{M_t}{M_\infty} = 1-\frac{6}{R_2^2}\sum_{n=1}^{\infty}\frac{1}{x_n\varphi(x_n)}\{\frac{1}{x_n}\left(\sin^2(R_1x_n)-\frac{R_1x_n}{2}\sin(2R_1x_n)\right)\sin[k(R_2-R_1)x_n] + \frac{1}{k}\left[R_2-\frac{1}{kx_n}\sin[k(R_2-R_1)x_n]-R_1\cos[k(R_2-R_1)x_n]\right]\sin^2(R_1x_n)\}\times\exp\left(-D_1x_n^2t\right). \tag{A19}$$

Yet, if $k(R_2 - R_1)/R_1$ is rational we have the additional terms of Eqs. (A15) and (A16) in the expressions of v_1 and v_2 that yield the following extra term in the fractional release solution of Eq. (A19)

$$-\frac{6}{\pi^2R_2^2(lk+m)}\sum_{n=1}^{\infty}\left\{\frac{R_1^2(-1)^{mn+(l+m)^n}}{n^2m}+\frac{k(R_2-R_1)\left[R_2-R_1(-1)^{nl}\right]}{n^2l}\right\}\times\exp\left(-\frac{D_1m^2n^2\pi^2}{R_1^2}t\right). \tag{A20}$$

Eqs. (3), (4) and (5) presented in Subsection 2.1, result from the Eqs. (A19), (A10) and (A20), respectively, if, for simplicity, we set $R_r = R_2/R_1$, $y_n = R_1x_n$, $\varphi_2(y_n) = y_n\varphi(y_n)$ and

$$\varphi_1(y_n) = \frac{1}{y_n}\left(\sin^2y_n-\frac{y_n}{2}\sin2y_n\right)\sin[ky_n(R_r-1)] + \frac{1}{k}\left\{R_r-\frac{1}{ky_n}\sin[ky_n(R_r-1)]-\cos[ky_n(R_r-1)]\right\}\sin^2y_n.$$

Note that in the limiting case $D_1 = D_2 = D$, where $k = 1$, the obtained fractional release reduces to the known result of the homogeneous sphere (see Eq. (4) of Ref. [32]). Indeed, suppose for simplicity that $R_r - 1$ is irrational, to consider the simple case of Eq. (3). In this case Eq. (4) gives $ysin(R_ry) = 0$ with positive roots $y = n\pi/R_r$, $n = 1$, 2,.... Then $\varphi_1 = R_rsin^2y_n$ and $\varphi_2 = R_ry_n^2sin^2y_n$. Therefore, Eq. (3) yields $\frac{M_t}{M_\infty} = 1-\frac{6}{R_r^2}\sum_{n=1}^{\infty}\frac{1}{y_n^2}\exp\left(-y_n^2\frac{D}{R_1^2}t\right) = 1-\frac{6}{\pi^2}\sum_{n=1}^{\infty}\frac{1}{n^2}\exp\left(-n^2\pi^2\frac{D}{R_2^2}t\right)$.

References

[1] C.-J. Kim, P.I. Lee, Composite poly(vinyl alcohol) beads for controlled drug delivery, Pharm. Res. 9 (1992) 10–16.
[2] R. Xu, X. Feng, W. Li, S. Xin, X. Wang, H. Deng, L. Xu, Novel polymer-layered silicate intercalated composite beads for drug delivery, J. Biomater. Sci. Polym. Ed. 24 (2013) 1–14.
[3] A. Streubel, J. Siepmann, N.A. Peppas, R. Bodmeier, Bimodal drug release achieved with multi-layer matrix tablets: transport mechanisms and device design, J. Control. Release 69 (2000) 455–468.
[4] S. De Koker, R. Hoogenboom, B.G. De Geest, Polymeric multilayer capsules for drug delivery, Chem. Soc. Rev. 41 (2012) 2867–2884.
[5] H. Nie, Y. Fu, C.-H. Wang, Paclitaxel and suramin-loaded core/shell microspheres in the treatment of brain tumors, Biomaterials 31 (2010) 8732–8740.
[6] M. Shi, Y.-Y. Yang, C.-S. Chaw, S.-H. Goh, S.M. Moochhala, S. Ng, J. Heller, Double walled POE/PLGA microspheres: encapsulation of water-soluble and water-insoluble proteins and their release properties, J. Control. Release 89 (2003) 167–177.
[7] E.C. Tan, R. Lin, C.-H. Wang, Fabrication of double-walled microspheres for the sustained release of doxorubicin, J. Colloid Interface Sci. 291 (2005) 135–143.
[8] D.N. Soulas, M. Sanopoulou, K.G. Papadokostaki, Performance of three-layer controlled release devices with uniform or non-uniform materials properties: experiment and computer simulation, J. Membr. Sci. 372 (2011) 1–10.
[9] D.N. Soulas, M. Sanopoulou, K.G. Papadokostaki, Proxyphylline release kinetics from symmetrical three-layer silicone rubber matrices: effect of different excipients in the outer and rate-controlling layers, Int. J. Pharm. 427 (2012) 192–200.
[10] S. Muschert, F. Siepmann, B. Leclercq, B. Carlin, J. Siepmann, Prediction of drug release from ethycellulose coated pellets, J. Control. Release 135 (2009) 71–79.
[11] W.C. Gunsel, R.G. Dusel, in: A.H. Lieberman, L. Lachman, J.B. Schwartz (Eds.), Pharmaceutical Dosage Forms: Tablets, Marcel Dekker Inc., New York, 1989.
[12] S. Parveen, R. Misra, S.K. Sahoo, Nanoparticles: a boon to drug delivery, therapeutics, diagnostics and imaging, Nanomedicine: NBM 8 (2012) 147–166.
[13] V.P. Torchilin, Recent advances with liposomes as pharmaceutical carriers, Nat. Rev. Drug Discov. 4 (2005) 145–160.
[14] S. Antimisiaris, C.A. Peptu, in: M. Popa, R.M. Ottenbrite, C.V. Uglea (Eds.), Medical Applications of Polymers, American Scientific Publishers, 2011.
[15] T.M. Allen, P.R. Cullis, Liposomal drug delivery systems: from concept to clinical applications, Adv. Drug Deliv. Rev. 65 (2013) 36–48.
[16] J.S. Lee, J. Feijen, Polymersomes for drug delivery: design, formation and characterization, J. Control. Release 161 (2012) 473–483.
[17] E.R. Gilles, J.M.J. Fréchet, Dendrimers and dendritic polymers in drug delivery, Drug Discov. Today 10 (2005) 35–43.
[18] M.K. Bijsterbosch, T.J.C. van Berkel, Native and modified lipoproteints as drug delivery systems, Adv. Drug Deliv. Rev. 5 (1990) 231–251.
[19] J. Siepmann, F. Siepmann, Modeling of diffusion controlled drug delivery, J. Control. Release 161 (2012) 351–362.
[20] T. Higuchi, Rate of release of medicaments from ointment bases containing drugs in suspension, J. Pharm. Sci. 50 (1961) 874–875.
[21] N.A. Peppas, Analysis of Fickian and non-Fickian drug release from polymers, Pharm. Acta Helv. 60 (1985) 110–111.
[22] P.L. Ritger, N.A. Peppas, A simple equation for description of solute release I. Fickian and non-Fickian release from non-swellable devices in the form of slabs, spheres, cylinders or discs, J. Control. Release 5 (1987) 23–36.
[23] J. Siepmann, H. Kranz, R. Bodmeier, N.A. Peppas, HPMC matrices for controlled drug delivery: a new model combining diffusion, swelling and dissolution mechanisms and predicting the release kinetics, Pharm. Res. 16 (1999) 1748–1756.
[24] K. Kosmidis, P. Argyrakis, P. Macheras, A reappraisal of drug release laws using Monte Carlo simulations: the prevalence of the Weibull function, Pharm. Res. 20 (2003) 988–995.
[25] V. Papadopoulou, K. Kosmidis, M. Vlachou, P. Macheras, On the use of the Weibull function for the discernment of drug release mechanisms, Int. J. Pharm. 309 (2006) 44–50.

[26] P. Macheras, A. Iliadis, Modeling in Biopharmaceutics, Pharmacokinetics, and Pharmacodynamics: Homogeneous and Heterogeneous Approaches, Springer, New York, 2006.
[27] K. Kosmidis, P. Argyrakis, P. Macheras, Fractal kinetics in drug release from finite fractal matrices, J. Chem. Phys. 119 (2003) 6373–6377.
[28] R. Villalobos, S. Cordero, A.M. Vidales, A. Domínguez, In silico study on the effects of matrix structure in controlled drug release, Phys. A 367 (2006) 305–318.
[29] K. Kosmidis, P. Macheras, Monte Carlo simulations for the study of drug release from matrices with high and low diffusivity areas, Int. J. Pharm. 343 (2007) 166–172.
[30] K. Kosmidis, P. Macheras, Monte Carlo simulations of drug release from matrices with periodic layers of high and low diffusivity, Int. J. Pharm. 354 (2008) 111–116.
[31] L. Martínez, R. Villalobos, M. Sánchez, J. Cruz, A. Ganem, L.M. Melgoza, Monte Carlo simulations for the study of drug release from cylindrical matrix systems with an inert nucleus, Int. J. Pharm. 369 (2009) 38–46.
[32] A. Hadjitheodorou, G. Kalosakas, Quantifying diffusion-controlled drug release from spherical devices using Monte Carlo simulations, Mater. Sci. Eng. C33 (2013) 763–768.
[33] S. Casault, G.W. Slater, Comments concerning: Monte Carlo simulations for the study of drug release from matrices with high and low diffusivity areas, Int. J. Pharm. 365 (2009) 214–215.
[34] L.L. Lao, N.A. Peppas, F.Y.C. Booey, S.S. Venkatraman, Modeling of drug release from bulk-degrading polymers, Int. J. Pharm. 418 (2011) 28–41.
[35] M.R. Rasmussen, T. Snabe, L.H. Pedersen, Numerical modelling of insulin and amyloglucosidase release from swelling Ca-alginate beads, J. Control. Release 91 (2003) 395–405.
[36] H.S. Carlslaw, J.C. Jaeger, Conduction of Heat in Solids, Oxford University Press, 1959.